

# Simplified methods for determining the ionic resistance in a porous electrode using linear voltammetry

Xianbo Jin, Juntao Lu\*

Department of Chemistry, Wuhan University, Wuhan 430072, China

Received 30 September 1999; received in revised form 10 April 2000; accepted 24 May 2000

## Abstract

Two simplified methods are proposed for determining the internal ionic resistance of a porous electrode using linear voltammetry in the double layer region. With the 70% current response time  $t_{0.7}$  on linear voltammogram and the independently measured uncompensated solution resistance  $R_e$ , the internal ionic resistance of a porous electrode can be calculated using the equation  $R_p = 2.483t_{0.7}/C_{\text{total}} - 2.989R_e$ , where  $C_{\text{total}}$  is the total capacitance of the porous electrode and can be deduced from the plateau current on the voltammogram. When  $R_p$  is not much smaller than  $R_e$ , it is also possible to estimate the ionic resistance according to the curve shape of the linear voltammogram without knowing  $R_e$ . © 2001 Elsevier Science B.V. All rights reserved.

**Keywords:** Porous electrode; Ionic resistance; Batteries; Linear voltammetry

## 1. Introduction

Porous electrodes have been widely used for decades in a variety of electrochemical techniques, such as batteries, fuel cells, electrolyses and electrochemical sensors mainly because of the advantages associated with their highly developed electrochemical surface areas. In general, however, not all the electrochemical surface in a porous electrode is uniformly utilized owing to the internal resistance [1]. In many cases, the porous electrode itself is made of highly conductive materials and the electronic resistance may be neglected compared with the ionic resistance. Therefore, the determination of the ionic resistance is a frequently encountered task in works involving porous electrodes.

For the electrodes which are thick and strong enough to be fixed in a frame, the classical four-point measurement is most straightforward for determining the internal ionic resistance. However, in many cases this approach is not realistic because the porous electrode is very thin and mechanically too weak to be framed, such as the catalytic layer of gas diffusion electrodes for fuel cells or air batteries. Similar situation happens to the active layer of lithium ion batteries where the active material is a thin porous layer adhered on a solid metal film. Besides, one often prefers in

situ to ex situ measurements because of reliability considerations. In fact, in some practical works even a rough in situ estimation of the ionic resistance would be very helpful for optimization of the electrode. It is, therefore, desirable to develop simple techniques for in situ determining the ionic resistance. These methods would be particularly useful for those involved in the practical works of battery research and development.

In 1990 Takahashi added a reversible redox couple to the solution and deduced the internal ionic resistance according to the well-established polarization theory for porous electrodes [2]. In a recent work related to the electrodes for the proton exchange membrane fuel cells, Boyer and coworkers inserted an inactive layer, which had the same structure as the catalytic layer, between the catalytic layer and the Nafion® membrane and estimated the ionic resistance of the catalytic layer according to the changes in polarization due to the inserted inactive layer [3]. However, these approaches are not in situ and less convenient.

Early in the 1970s, Austin and Gagnon used a series expression to describe the current response of a porous electrode to linear potential scanning in the double layer region in the presence of uncompensated solution resistance [4,5]. With independently measured uncompensated resistance  $R_e$ , they were able to deduce the double layer capacitance and the internal ionic resistance by curve fitting. Based on the structural parameters of the porous electrode, the ionic resistance thus obtained was thought to be reason-

\* Corresponding author. Tel.: +86-27-764-7617; fax: +86-27-764-7617.  
E-mail address: jtl@whu.edu.cn (J. Lu).

able, but no attempt was made to check with a direct four-point measurement. Zhou deduced an equation describing the linear voltammetry of a porous electrode in the double layer region in the absence of uncompensated ionic resistance but did not apply this equation to determine the internal ionic resistance though it has the potential [6]. From numerical studies of these equations we found it possible to replace the tedious computer curve fitting with a simple arithmetic calculation. With separately measured uncompensated solution resistance, the internal resistance of the porous electrode can be deduced from the 70% current response time  $t_{0.7}$  using a very simple linear equation. In favorable circumstances it was found still possible to estimate the internal ionic resistance according to the line shape of the linear voltammogram without knowing  $R_e$ . These developments make the linear voltammetry a very convenient tool for the determination of the ionic resistance in a porous electrode. In this paper, we first present the results of numerical studies which serve as the basis for the proposed methods and then report experimental data to compare the  $R_p$  values obtained using the simplified methods with those obtained using the four-point measurement.

## 2. Experimental

In order to test the proposed method described below, a porous silver disk electrode in alkaline solution (0.5 mol/l KOH) was used as the model system. The electrode was made from the silver powder for zinc-silver batteries by pressing in a mold. The porous silver electrode was a disk 1.30 cm in diameter and 3.24 mm thick. The porosity of the test electrode was found to be 0.649 according to its weight and apparent volume. The test electrode was intentionally made thick so that the response time was relatively long and the experiment could be easily carried out without the need for fast response equipment. The test electrode was tightly sealed in a Teflon frame and clamped between the two half cells of the four-point measurement device. Each of the half cells contains an auxiliary electrode and a Luggin capillary reaching the test sample.

In the four-point measurements, a current was applied through the auxiliary electrodes located on the two sides of the porous silver disk and the potential difference  $\Delta E$  between the two capillaries was recorded as a function of the current  $I$ . The ionic resistance between the two capillaries was calculated from the slope  $R=dE/dI$ . The uncompensated resistance between the capillary and the silver electrode  $R_e$  were obtained according to the sudden potential change of the test electrode (on an oscilloscope) following a current step passing through the test electrode and an auxiliary electrode. The ionic resistance of the porous electrode was then calculated to be  $R_p=R-R_{e1}-R_{e2}$ , where  $R_{e1}$  and  $R_{e2}$  are the uncompensated resistances between the test electrode and the capillaries on the two sides, respectively.

To test the effects of  $R_e$  on the determination of  $R_p$ , the distance between the capillary and the test electrode was set at different values. To ensure comparability, the linear potential scanning measurements were conducted with exactly the same test electrode and in the same device as for the four-point measurements. Linear potential scanning was carried out with a potentiostat and recorded on an  $x$ - $y$  recorder in the potential region from  $-0.40$  to  $-0.35$  V (versus Ag/Ag<sub>2</sub>O in the same solution) where the double layer capacity is constant within experimental error. Before each potential scanning, the potential was kept at the starting value for a sufficient time (about a minute) to reach a uniform potential distribution within the porous electrode.

## 3. Numerical analyses of the linear voltammetry for porous electrodes

### 3.1. In the absence of uncompensated solution resistance ( $R_e=0$ )

The most popular approach to analyze the polarization of porous electrodes is based on a macroscopically homogeneous model. In this model, the porous electrode consists of two interpenetrated networks, i.e. the ionically conductive one (the liquid phase) and the electronically conductive one (the solid phase). The elemental sizes of the electrolyte pores and solid particles are much smaller than the thickness of the electrode but the pore diameters are greater than the double layer thickness. These macroscopically homogeneous electrodes can be characterized by so-called effective parameters such as effective specific resistance  $\rho$  ( $\Omega$  cm) and effective specific capacitance ( $F/cm^3$ ). To simplify the relevant equations, it is assumed in the following sections that the current in the electrolyte phase reaches the working electrode from a single side only of the electrode.

When the uncompensated solution resistance  $R_e$  is negligible compared with ionic resistance inside the electrode  $R_p$ , the dimensionless linear voltammogram in the double layer region has been deduced by Zhou [6]:

$$\beta = 2 \left( \frac{1}{\rho CL^2} \right)^{1/2} \left\{ \left( \frac{t}{\pi} \right)^{1/2} \left[ 1 + 2 \sum_{n=1}^{\infty} (-1)^n \exp \left( \frac{-n^2 \rho CL^2}{t} \right) \right] - 2(\rho CL^2)^{1/2} \sum_{n=1}^{\infty} \left[ (-1)^n \operatorname{erfc} \left( \frac{n^2 \rho CL^2}{t} \right)^{1/2} \right] \right\} \quad (1)$$

$$\beta = \frac{I}{\nu CLA} \quad (2)$$

where  $I$  is the electrical current (A),  $\nu$  the potential scan rate (V/s),  $C$  the double layer capacity per unit volume ( $F/cm^3$ ),  $L$  and  $A$  are the thickness (cm) and apparent area ( $cm^2$ ) of the porous electrode.  $\rho CL^2$  is a characteristic time for the porous electrode.  $\beta$  and  $t/\rho CL^2=T$  are the dimensionless current and time, respectively. When  $T$  is sufficiently large,  $\beta$  reaches essentially unity and the current levels off to the plateau

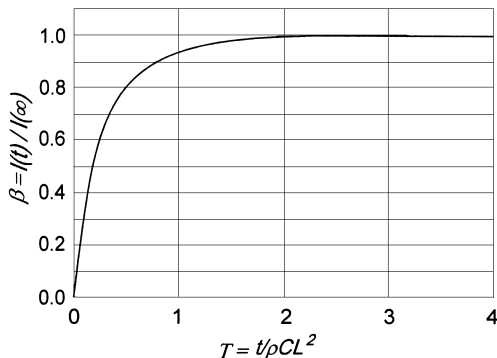


Fig. 1. Dimensionless linear voltammogram of a porous electrode in the double layer region in the absence of uncompensated solution resistance.

current  $I_C$ . The result of numerical calculations is shown in Fig. 1. From the plateau current  $I_C$  and scan rate  $v$ , the total capacitance can be readily obtained:  $C_{\text{total}} = CLA = I/v$ . We define a dimensionless time  $T_\beta = t_\beta / \rho CL^2$  for the current corresponding to  $\beta$  (i.e. a  $\beta$  fraction of the plateau current). From Fig. 1 the values of  $T$  for  $\beta = 0.9$  and  $0.7$ , denoted  $T_{0.9}$  and  $T_{0.7}$ , are found to be 0.848 and 0.403, respectively. When  $T = 2.30$ ,  $\beta$  essentially reaches unity (0.996). With previously determined value for  $C_{\text{total}}$  and the value of  $t_\beta$  taken from experimental voltammogram, the ionic resistance can be calculated:  $R_p = \rho LA = t_\beta / T_\beta C_{\text{total}}$ . For example, we may use the data point of 70% current response ( $\beta = 0.7$ ) to deduce  $R_p$ . In doing so, we first locate the point on the experimental linear voltammogram and take the corresponding time  $t_{0.7}$ . From Fig. 1,  $T_{0.7}$  can be found to be 0.403 and then  $R_p = t_{0.7} / T_{0.7} C_{\text{total}} = t_{0.7} / 0.403 C_{\text{total}} = 2.483 t_{0.7} / C_{\text{total}}$ . When this method is to be adopted, it is necessary to check whether the condition  $R_e = 0$  is met to a good approximation. The judgment can be made according to the shape of the rising part of the curve. A simple way for checking is to use a few representative data points. In practice, we found it convenient to use the time ratio  $T_{0.9} / T_{0.5} = t_{0.9} / t_{0.5}$  which should be close to 4.312 if  $R_e$  is negligible. The effects of  $R_e$  on the curve shape will be addressed in detail in the next section.

### 3.2. In the presence of uncompensated solution resistance $R_e$

Austin and Gagnon [4] reported the equations of linear voltammetry for a porous electrode in the double layer region in the presence of uncompensated solution resistance:

$$\beta = 1 - \sum_{n=1}^{\infty} \exp\left(-m_n^2 \frac{t}{\rho CL^2}\right) \left\{ \frac{2\psi^2}{[m_n^2(\psi^2 + m_n^2 + \psi)]} \right\} \quad (3)$$

where

$$\psi = \frac{\rho L}{AR_e} = \frac{R_p}{R_e} \quad (3a)$$

$$m_n \tan m_n = \psi \quad (3b)$$

the  $m_n$  values are the positive roots of equation  $m_n \tan m_n = \psi$ . Eq. (3) is a complicated function whose curve

fitting needs rather involved programming and is time consuming. When  $\psi$  is very small, namely the internal ionic resistance  $R_p$  being negligible compared with the uncompensated solution resistance  $R_e$ , Eq. (3) reduces to the simple formula for a circuit consisting of resistance  $R_e$  and capacitance  $C_{\text{total}} (=CLA)$  connected in series:

$$\beta = 1 - \exp\left(\frac{-t}{R_e C_{\text{total}}}\right) \quad (4)$$

In the situation described by Eq. (4), the linear voltammogram contains no information of  $R_p$  and, therefore, is not applicable for  $R_p$  determination. On the other extreme where  $R_e = 0$ , Eq. (4) reduces to

$$\beta = 1 - \frac{8}{\pi^2} \sum_{n=1}^{\infty} \left[ \frac{(-1)^n}{(2n+1)^2} \right] \exp\left[ \frac{-(2n+1)^2 \pi^2 t}{\rho CL^2} \right] \times \sin\left[ \frac{(2n+1)}{2\pi} \right] \quad (5)$$

As proved by our numerical calculations, Eq. (5) is equivalent to Eq. (1).

It is seen from Eq. (3) that the value of  $\psi$  determines the shape of the current response curve. Conversely, one may deduce the  $\psi$  value and, in turn, the  $R_p$  value from the curve shape. The effect of  $\psi$  can be best shown with dimensionless plots. To include the curves for  $\psi$  ranging from 0 to infinity and give all the curves in a fully developed version, the  $\psi$  values are divided into two regions and plotted separately using two different characteristic times as shown in Fig. 2 (characteristic times  $\rho CL^2$  and  $R_e CLA = R_e C_{\text{total}}$  for Fig. 2a and b, respectively). For comparison, the scales of Fig. 2a and b were sized so that the curves for  $\psi = 1$  in the two figures appear identical. It is seen that the curve shape changes with  $\psi$ . A simple way to characterize the curve shape is to use the ratio of the times at different  $\beta$  values. We found the time ratio  $t_{0.9}/t_{0.5} = T_{0.9}/T_{0.5}$  suitable for the curve shape characterization and will use it in the following sections. Fig. 3 indicates that the change in curve shape mainly takes place in the region of  $\psi$  values 0.3–30. When  $\psi > 100$ , the dimensionless current response curves ( $\beta$  curves) are essentially identical to that for infinite  $\psi$ . In these cases, the influence of  $R_e$  on the determination of  $R_p$  is negligible. Therefore, if  $t_{0.9}/t_{0.5}$  is found to be close to 4.3 (i.e.  $\psi$  being sufficiently large) one can simply use the method described in Section 3.1. On the other hand, if  $t_{0.9}/t_{0.5}$  is close to 3.32 (corresponding to  $\psi < 0.1$ ),  $R_p$  will be too small compared with  $R_e$  to be extracted with reasonable accuracy. For acceptable results,  $\psi$  should be no less than 0.1.

### 3.3. $T_\beta \psi - \psi$ relations

According to the definitions of  $T_\beta$  and  $\psi$ ,  $T_\beta \psi$  is an experimentally accessible value:

$$T_\beta \psi = \frac{t_\beta}{R_e C_{\text{total}}} \quad (6)$$

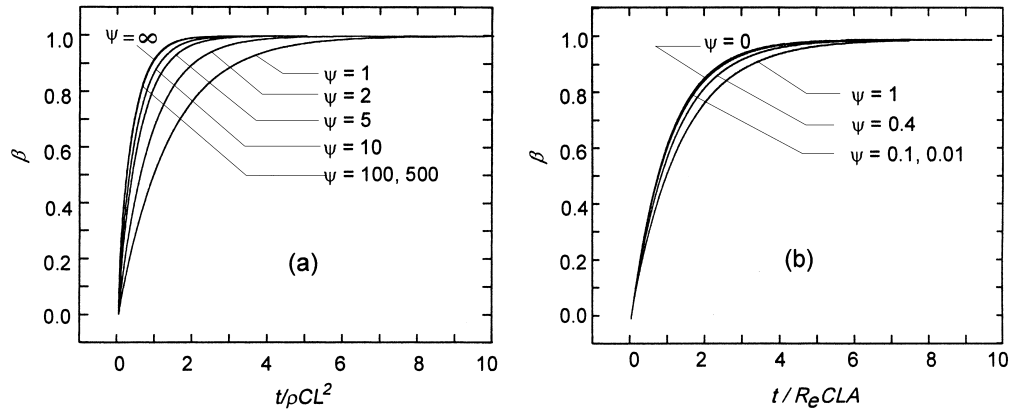


Fig. 2. Dimensionless linear voltammograms in the presence of uncompensated solution resistance: (a)  $\infty > \psi > 1$ ; (b)  $1 > \psi > 0$ .

where  $t_\beta$  is directly taken from the linear voltammogram when the value for  $\beta$  has been chosen;  $R_e$  and  $C_{total}$  are determined the way described in previous sections. If the relation between  $T_\beta\psi$  and  $\psi$  is established, then  $\psi$  and, in turn,  $R_p$  can be deduced from the experimental  $T_\beta\psi$ . It is found in numerical studies that the  $T_\beta\psi$ – $\psi$  relations for  $\beta$  values between 0.5 and 0.9 are roughly linear and can be approximately described with a general formula:

$$T_\beta\psi = a_\beta + b_\beta\psi \quad (7)$$

where  $a_\beta$  and  $b_\beta$  are constants for a fixed  $\beta$ . Multiplying both sides of Eq. (7) with  $(\rho CL^2/\psi)$  results in

$$\rho CL^2 T_\beta = \left( a_\beta R_e + \frac{b_\beta \rho L}{A} \right) CLA \quad (8)$$

or

$$t_\beta = R_p C_{total} T_\beta = (a_\beta R_e + b_\beta R_p) C_{total} \quad (8a)$$

It is interesting that Eq. (8a) appears similar to the formula of the characteristic time for an equivalent circuit consisting of two resistors ( $a_\beta R_e$  and  $b_\beta R_p$ ) and a capacitor connected in series. The approximate linearity of Eq. (7) is shown in Fig. 4a. A careful check on the  $T_\beta\psi$ – $\psi$  relations would find that they are not strictly linear as proved by the changes of slope ( $d(T_\beta\psi)/d\psi$ ) with respect to  $\psi$  (Fig. 4b). Fortunately, the slope for  $\beta=0.7$  turns out to be a constant with satisfactory precision over a wide region of  $\psi$  values (0.02–500):

$$T_{0.7}\psi = 1.2040 + 0.4028\psi \quad (9)$$

Substituting  $R_p=R_e\psi$  and  $T_{0.7}\psi=t_{0.7}/R_e C_{total}$  (Eq. (6)) into Eq. (9) results in

$$R_p = \frac{2.483t_{0.7}}{C_{total}} - 2.989R_e \quad (10)$$

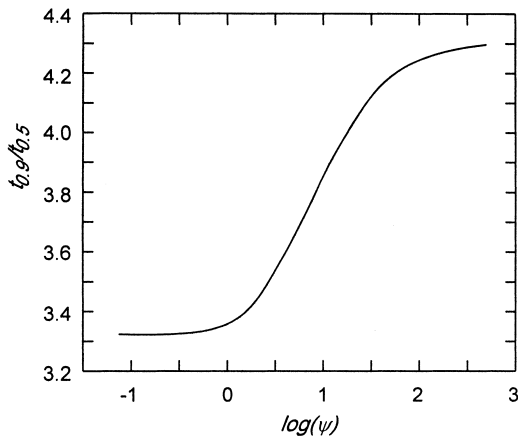


Fig. 3. Plot of  $t_{0.9}/t_{0.5}$  against  $\log(\psi)$ .

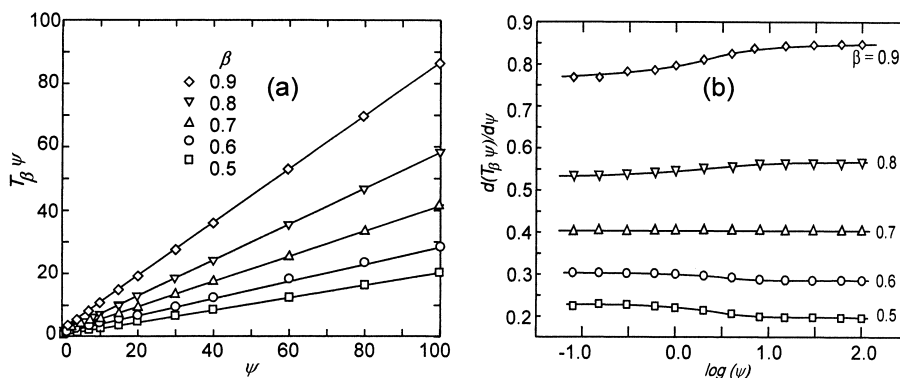


Fig. 4. Approximate linearity of  $T_\beta\psi$  vs.  $\psi$ : (a)  $T_\beta\psi$  vs.  $\psi$ ; (b)  $d(T_\beta\psi)/d\psi$  vs.  $\psi$ .

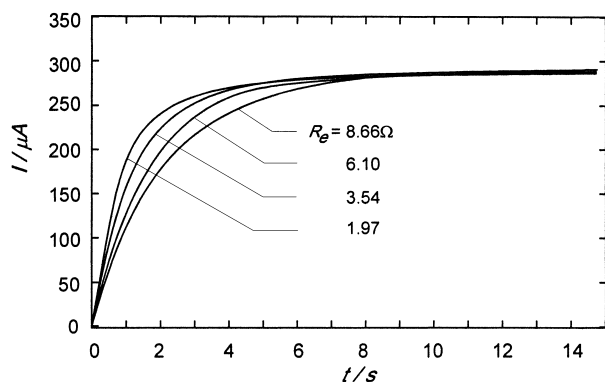


Fig. 5. Experimentally measured linear voltammograms at scan rate 1.67 mV/s for different uncompensated solution resistances.

In fact, Eq. (10) was found to well fit the theoretical values for the two extremes. For  $R_e=0$  ( $\psi=\infty$ ), Eq. (10) gives  $t_{0.7}=0.4028 R_p C_{\text{total}}$  which turns out to be in good agreement with the result of numerical calculation ( $0.4028 R_p C_{\text{total}}$  for  $t_{0.7}$ ) of Eqs. (1) and (5). On the other hand, for the case of  $R_p$  being negligible compared with  $R_e$  ( $\psi=0$ ), Eq. (10) becomes  $t_{0.7}=1.2040 R_e C_{\text{total}}$ , in excellent agreement with Eq. (4) ( $1.2040 R_e C_{\text{total}}$  for  $t_{0.7}$ ). From the experimental values for  $t_{0.7}$ ,  $R_e$  and  $C_{\text{total}}$ , the internal ionic resistance  $R_p$  can be readily obtained using Eq. (10).

## 4. Results and discussion

### 4.1. Determining $R_p$ with known $R_e$

To test the method developed in the previous section, linear potential scan was carried out for the same porous electrode at different  $R_e$  values. A few of the current response curves are given in Fig. 5. As expected, the current rising became slower with increasing  $R_e$ . The  $R_e$  values were separately measured as mentioned above. The plateau current was reproducible within  $\pm 1\%$  and slightly sloped due probably to residual Faradaic current which was corrected for as a baseline shift in data processing. From the plateau current  $I_C=0.280$  mA and scan rate  $v=1.67$  mV/s, the total capacitance  $C_{\text{total}}$  was found to be 0.168 F.

In Table 1, the  $t_{0.7}$  values were directly read from the experimental  $I-t$  curves. From 10 experimental runs at different  $R_e$  values, the  $R_p$  values were calculated from Eq. (10) with an average  $10.5 \pm 0.3 \Omega$ , in good agreement with the value  $10.3 \pm 0.3 \Omega$  found by the four-point measure-

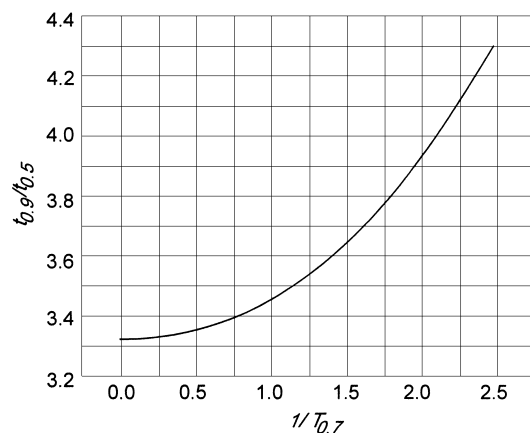


Fig. 6. The working curve of  $t_{0.9}/t_{0.5}$  vs.  $1/T_{0.7}$ .

ments. Eq. (10) indicates that if  $\psi(=R_p/R_e)$  is much smaller than unity,  $R_p$  will be a small difference between two large numbers and will have fewer effective digits. Usually,  $\psi$  should be no less than 0.1 in practice. On the contrary, if  $\psi$  is much larger than unity, the last term in Eq. (10) becomes only a small correction. When  $\psi=100$ , for example, this term presents only a correction of 2.4% which could be neglected for most practical works. The  $\psi$  values in Table 1 range roughly from 1 to 5.5 which are in the proper region for deducing  $R_p$ .

### 4.2. Estimation of $R_p$ without knowing $R_e$

In the experiments described in Section 4.1, the uncompensated solution resistance  $R_e$  had been separately measured as a known parameter. However, in favorable situations it is still possible to obtain  $R_p$  without knowing  $R_e$ . Combining Fig. 3 and Eq. (9), a working curve relating  $t_{0.9}/t_{0.5}$  and  $T_{0.7}$  can be established as shown in Fig. 6. After taking  $t_{0.9}$  and  $t_{0.5}$  from the experimental linear voltammogram,  $T_{0.7}$  can be readily found from Fig. 6. Finally,  $R_p$  can be calculated:

$$R_p = \frac{t_{0.7}}{(T_{0.7} C_{\text{total}})} \quad (11)$$

Table 2 lists the  $R_p$  data obtained using Eq. (11) based on the same measurements as in Table 1. In Table 2, the  $R_e$  values are deduced using equation  $R_e=R_p/\psi$  where the  $\psi$  value was found from the experimental  $t_{0.9}/t_{0.5}$  using Fig. 3. The statistics over the 10 experimental runs gave a  $R_p$  value  $11.3 \pm 0.7 \Omega$ . The average value is about 10% higher than that from the four-point measurement and the standard

Table 1  
Deducing  $R_p$  from  $t_{0.7}$  and  $R_e$

Experimental run	1	2	3	4	5	6	7	8	9	10
$R_e/\Omega$ ( $\pm 0.03$ )	1.97	2.76	3.54	4.25	5.43	6.10	7.24	8.66	10.35	12.60
$t_{0.7}/s$ ( $\pm 0.02$ )	1.11	1.26	1.45	1.58	1.81	1.98	2.20	2.45	2.78	3.27
$R_p/\Omega$	10.5	10.3	10.8	10.6	10.4	10.9	10.8	10.2	10.0	10.5

Table 2  
Deducing  $R_p$  and  $R_e$  from  $t_{0.9}/t_{0.5}$

Experimental run	1	2	3	4	5	6	7	8	9	10
$t_{0.9}/s (\pm 0.02)$	2.30	2.54	2.95	3.14	3.52	3.91	4.33	4.81	5.43	6.21
$t_{0.5}/s (\pm 0.02)$	0.62	0.70	0.83	0.88	1.02	1.13	1.26	1.42	1.61	1.85
$t_{0.9}/t_{0.5}$	3.71	3.63	3.55	3.56	3.45	3.46	3.44	3.39	3.38	3.37
$\psi$	5.45	4.20	3.30	3.34	1.97	2.04	1.83	1.23	1.15	0.97
$R_p/\Omega$	10.7	10.8	11.0	12.1	10.3	11.8	12.3	10.5	11.3	11.8
$R_e/\Omega$	1.96	2.58	3.32	3.68	5.24	5.80	6.73	8.59	9.90	12.2

deviation is about two times that in the previous section. The main source of standard deviation is thought to be the low sensitivity of  $t_{0.9}/t_{0.5}$  to  $\psi$  and, in turn, the high sensitivity of  $1/T_{0.7}$  to  $t_{0.9}/t_{0.5}$ . It is seen from Fig. 6 that an 1% error in  $t_{0.9}/t_{0.5}$  would cause an error of about 5% in  $1/T_{0.7}$  in the region around  $t_{0.9}/t_{0.5}=4.0$ . For smaller  $t_{0.9}/t_{0.5}$  values, the situation would be worse. When  $t_{0.9}/t_{0.5}$  is below 3.4, it will be very difficult to find the correct value for  $1/T_{0.7}$ . On the contrary, the situation could be considered favorable if  $t_{0.9}/t_{0.5}$  is above 4. However, it should be noted that the maximum value for  $t_{0.9}/t_{0.5}$  (corresponding to  $\psi=\infty$ ) is 4.312. If  $t_{0.9}/t_{0.5}$  is found to be markedly larger than the maximum, the data should be considered not reliable or the macroscopically homogeneous model is not valid for the particular case studied.

## 5. Summary

The internal ionic resistance  $R_p$  of a porous electrode can be deduced from linear voltammogram and independently

measured uncompensated solution resistance  $R_e$  using a simple linear equation. For better result, the ratio of  $R_p/R_e=\psi$  should be above 0.1. Under favorable conditions it is possible to deduce  $R_p$  without knowing  $R_e$ , but the result will be less accurate. These methods are applicable to systems satisfying the conditions for the macroscopically homogeneous model with a potential region where the double layer capacitance is constant.

## References

- [1] N. Ibl, in: E. Yeager, J.O'M. Bockris, S. Sarangapani (Eds.), *Comprehensive Treatise of Electrochemistry*, Vol. 6, Plenum Press, New York, 1983 (Chapter 4).
- [2] K.M. Takahashi, *J. Electrochem. Soc.* 137 (1990) 3850.
- [3] C. Boyer, S. Gamburgzev, O.A. Velev, S. Srinivasan, A.J. Appleby, *Electrochim. Acta* 43 (1998) 3703.
- [4] L.G. Austin, E.G. Gagnon, *J. Electrochem. Soc.* 120 (1973) 251.
- [5] E.G. Gagnon, *J. Electrochem. Soc.* 120 (1973) 1052.
- [6] W. Zhou, *Electrochemical Measurements*, Shanghai Science & Technology Press, Shanghai, 1985, pp. 120–123.